Stem Cell Reports, Volume *17*

Supplemental Information

Stabilization of cell-cell adhesions prevents symmetry breaking and locks in pluripotency in 3D gastruloids

Federica Cermola, Filomena Amoroso, Federica Saracino, Eduardo Ibello, Dario De Cesare, Annalisa Fico, Gilda Cobellis, Enrica Scalera, Costanza Casiraghi, Cristina D'Aniello, Eduardo Jorge Patriarca, and Gabriella Minchiotti

SUPPLEMENTAL INFORMATION

Figures S1-S6

Tables S3-S4

Experimental Procedures

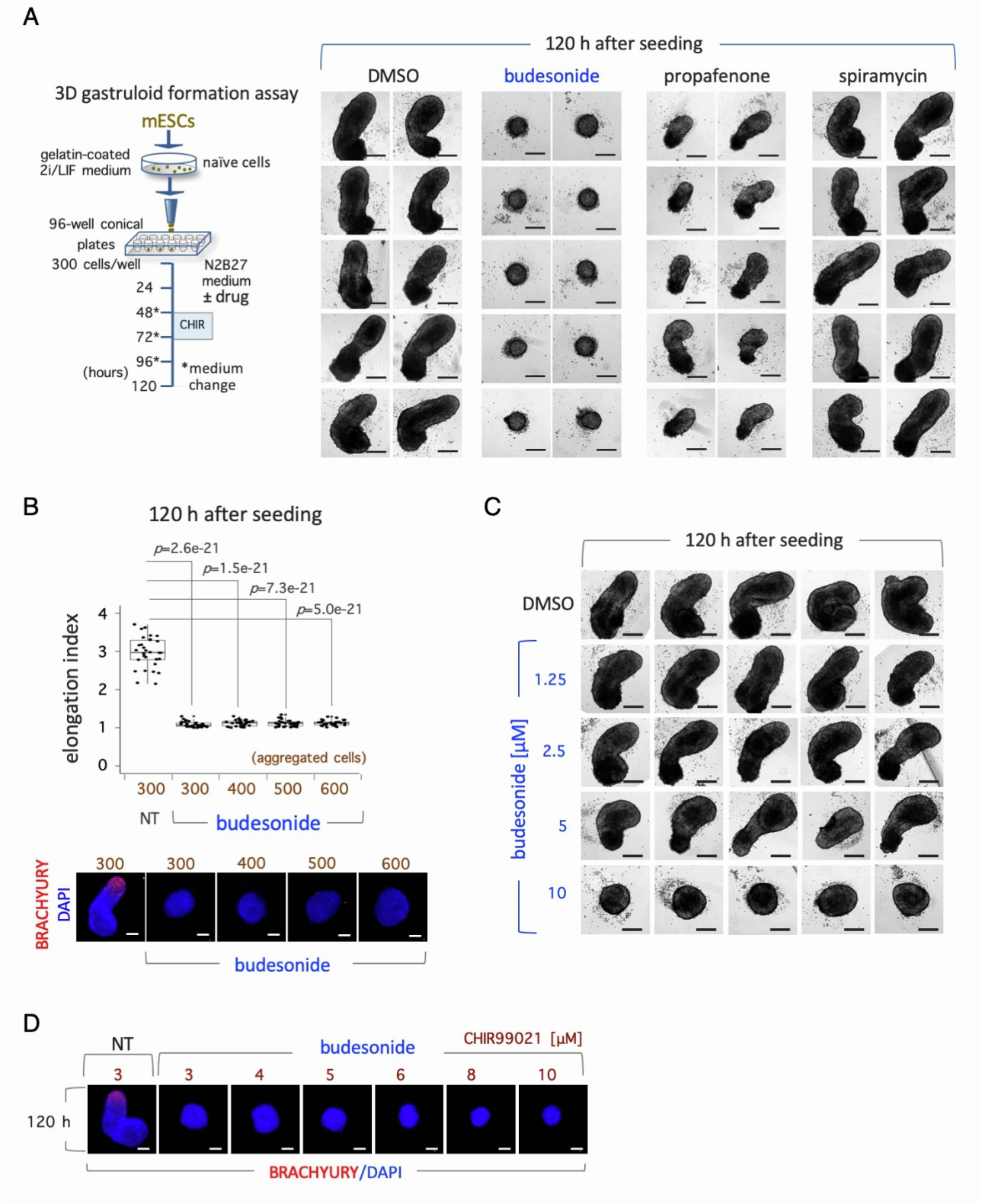

SUPPLEMENTARY FIGURE 1

Figure S1. Effect of esMT inhibitors, aggregate cell number, and CHIR99021 concentration on gastruloid development.

(A) Schematic representation of the experimental design. 2i/LIF ESCs were plated on 96-well ultra-low attachment conical plates in N2B27 medium. Representative bright-field images of naïve ESCs -derived gastruloids (120 h) treated with DMSO (control) or the indicated drugs (budesonide, propafenone and spiramycin). The drugs were used at 10 μM and maintained throughout the experiment (bar, 100 μm).

(B) Effect of increased number of aggregated cells (300→600) on budesonide-dependent inhibition of gastruloid formation. Boxplot diagram of the elongation index of control (NT, not-treated with budesonide) and budesonide-treated gastruloids (120 h) (*top*). Representative confocal images of BRACHYURY (*red*) expression in gastruloids ± budesonide (120 h) (*bottom*). Nuclei were counterstained with DAPI (*blue*) (bar, 100 μm).

(C) Dose-dependent effect of budesonide on gastruloid elongation. Representative bright-field images of control (DMSO) and budesonide (1.25→10 μM) -treated gastruloids (bar, 50 μm).

(D) Dose-dependent effect of CHIR99021 on development of budesonide-treated gastruloids. Representative confocal images of BRACHYURY (*red*) expression in 120 h gastruloids ± budesonide (10 μM) ± CHIR99021 (3→10 μM). Nuclei were counterstained with DAPI (*blue*) (bar, 100 μm).

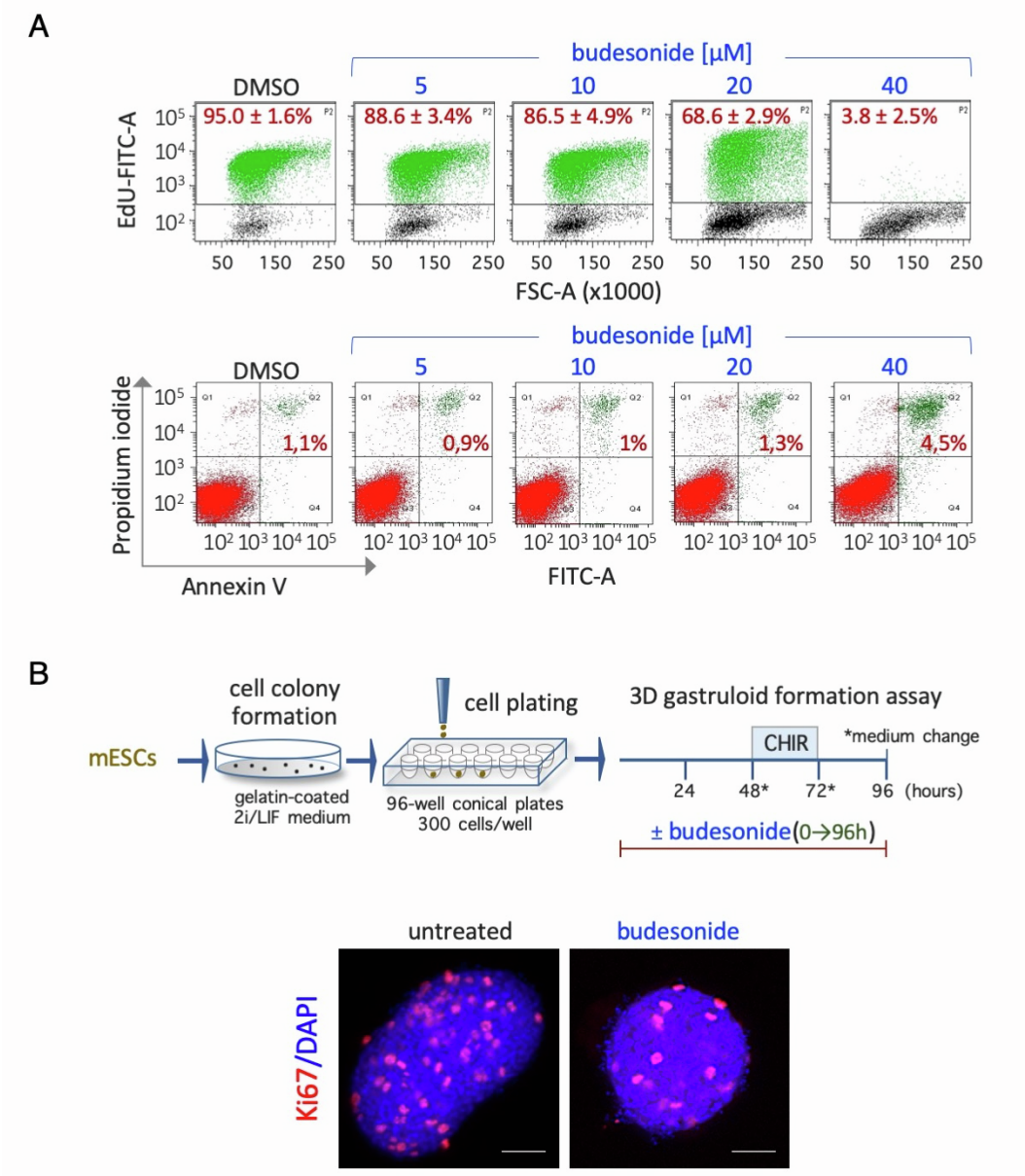

SUPPLEMENTARY FIGURE 2

Figure S2. Dose-dependent effect of budesonide on ESC proliferation and apoptosis.

(A) Representative FACS plot showing EdU^+ (*top*) and Annexin V/$Propidium^+$ (AV^+/PI^+, *bottom*) cells in FBS/LIF ESCs ± budesonide (5→40 μM) at 48 h (data are expressed as mean ± SD; n = 3).
(B) Schematic representation of the experimental design (*top*). Representative confocal images of Ki67 (*red*) expression in gastruloids ± budesonide (10 μM; bottom). Nuclei were counterstained with DAPI (*blue*) (bar, 50 μm).

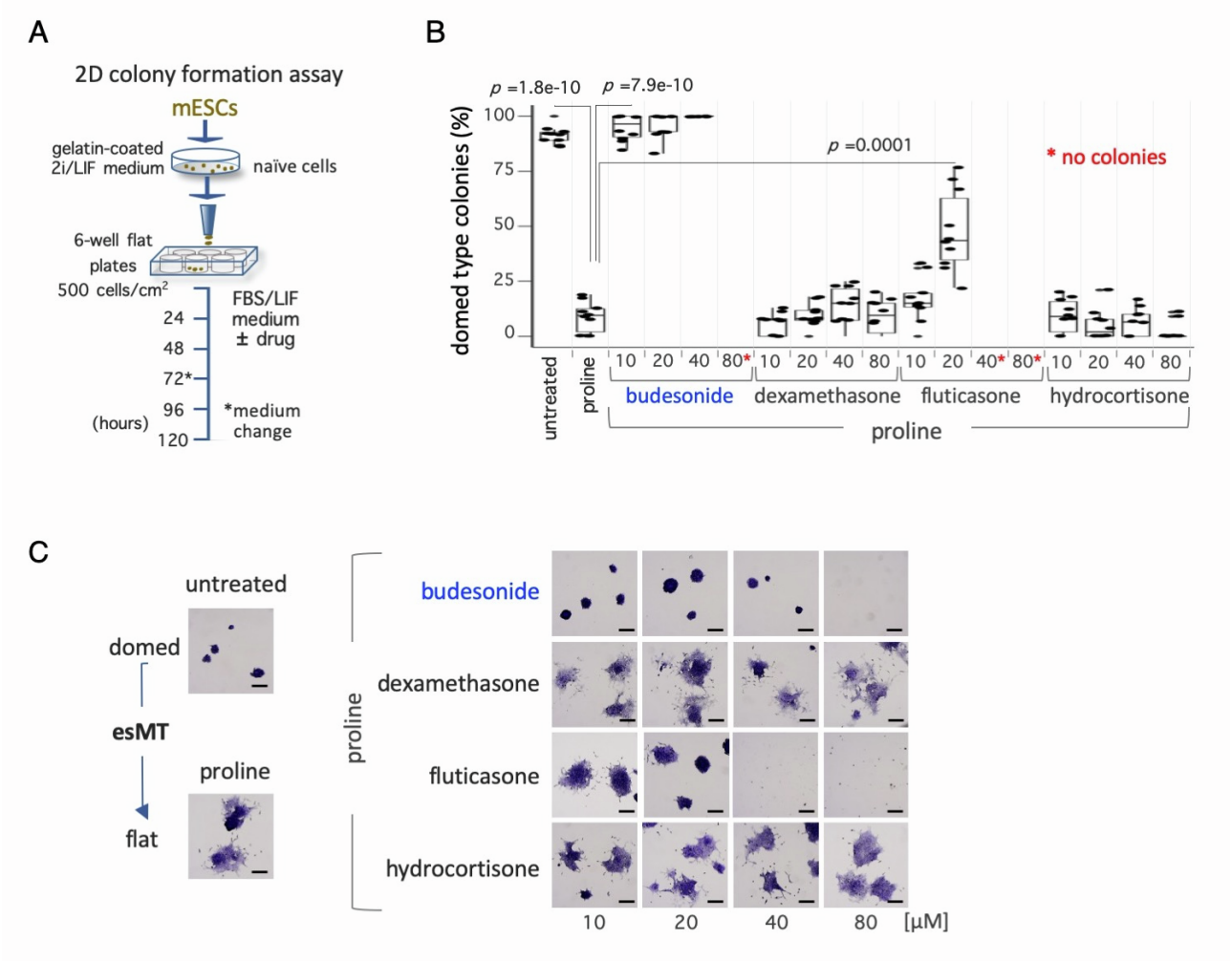

SUPPLEMENTARY FIGURE 3

Figure S3. Dose-dependent effects of glucocorticoids on esMT.

(A) Schematic representation of the experimental design. Naïve ESCs were plated (500 cell/cm^2) in FBS/LIF medium plus proline (500 μM) ± drugs at the indicated concentrations.

(B) Boxplot diagram showing the fraction (%) of domed-shaped colonies generated in FBS/LIF ± proline ± budesonide, dexamethasone, fluticasone or hydrocortisone at the indicated concentrations (10→80 μM). Red asterisks indicate absence of colonies (n = 2; 10 fields/condition).

(C) Representative bright-field images of crystal violet-stained cell colonies in the different culture conditions (bar, 200 μm).

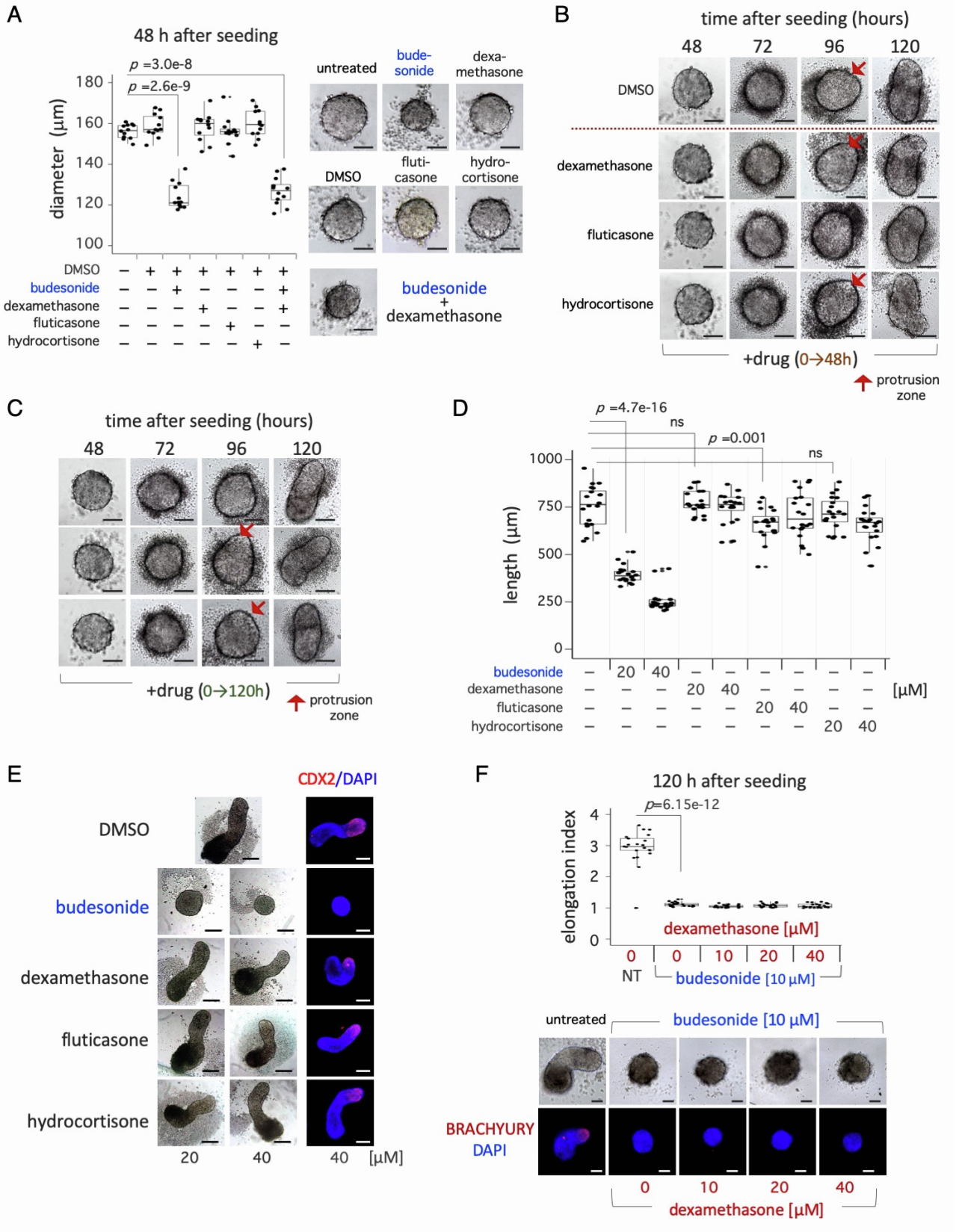

SUPPLEMENTARY FIGURE 4

Figure S4. Effect of typical glucocorticoids on gastruloid development.

(A) Boxplot diagram of the diameter distribution (*left)* and representative bright-field images (*right*) of the cell aggregates at 48 h, treated with either the indicated drugs, with DMSO or untreated (bar, 100 μm). The drugs were used either alone or in combination and at a final concentration of 10 μM each (n = 3; 12 aggregates/condition; bar, 100 μm).

(B) Time course representative bright-field images of gastruloids transiently (0→48 h) treated with dexamethasone, fluticasone or hydrocortisone (10 μM). DMSO was used as a control. Arrows indicate apical protrusion zone (bar, 100 μm).

(C) Time course representative bright-field images of gastruloids treated with dexamethasone, fluticasone or hydrocortisone (10 μM) from 0→120 h. DMSO was used as control. Arrows indicate apical protrusion zone (bar, 100 μm).

(D) Dose-dependent effect of glucocorticoids on gastruloid development. Boxplot diagram showing the length of aggregates/gastruloids (120 h) following the indicated treatments (n = 3; 20 gastruloids/condition).

(E) Representative bright-field images of budesonide, dexamethasone, fluticasone or hydrocortisone-treated gastruloids (120 h). The drugs were used at 20 and 40 μM (bar, 100 μm) (*left* and *middle panels*). Representative confocal images of CDX2 (*red*) expression in budesonide, dexamethasone, fluticasone or hydrocortisone (40 μM)-treated gastruloids (120 h) (*right panels*). Nuclei were counterstained with DAPI (*blue*) (bar, 100 μm).

(F) Boxplot diagram of the elongation index of gastruloids ± budesonide (10 μM) and increasing concentration of dexamethasone (10→40 μM) (*top*) (n = 3; 20 gastruloids/condition). Representative bright-field images and confocal images (*bottom*) of gastruloids (120 h) treated with budesonide (10 μM) ± increasing concentration of dexamethasone (10→40 μM) (bar, 50 μm). BRACHYURY expression (*red*) is shown. Nuclei were counterstained with DAPI (*blue*) (bar, 50 μm).

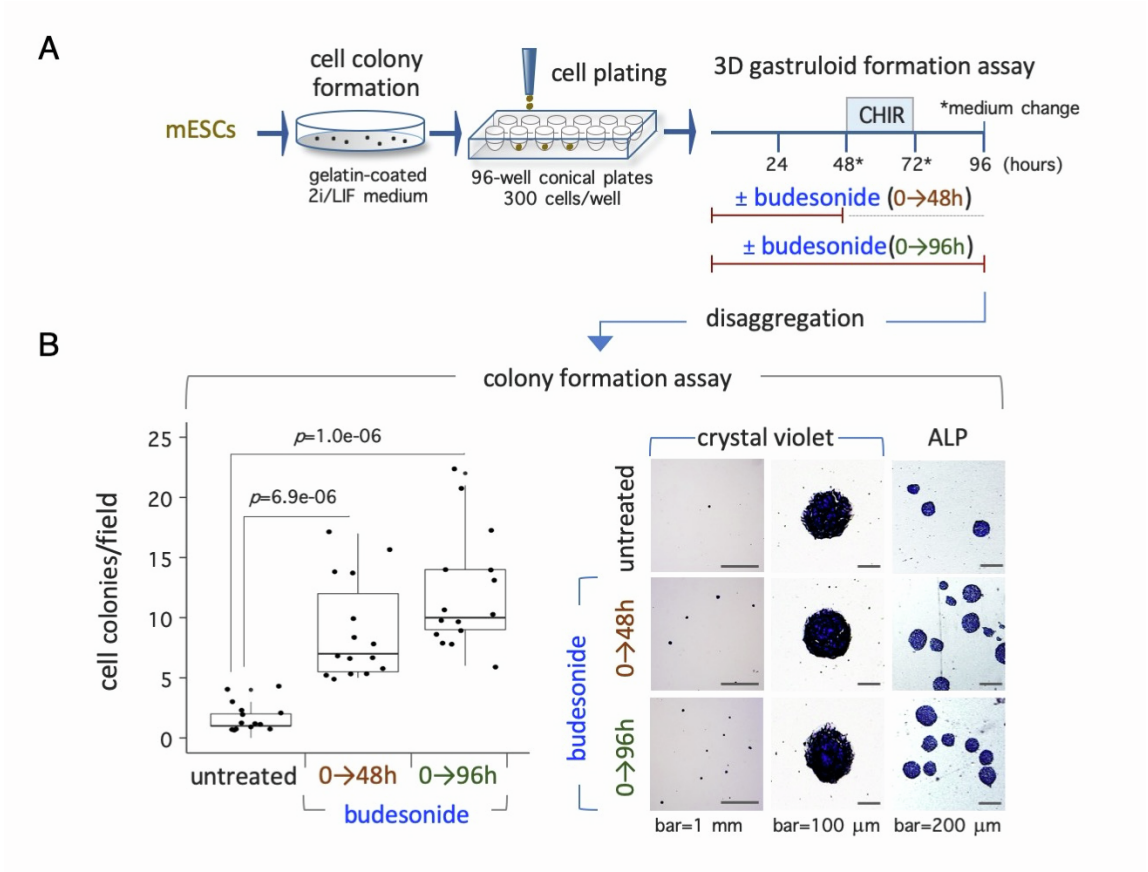

SUPPLEMENTARY FIGURE 5

Figure S5. Effect of budesonide on ESC self-renewal.

(A) Schematic representation of the experimental design. Control and budesonide-treated gastruloids were dissociated by trypsin digestion and the cells plated in FBS/2i/LIF medium at either 150 cells/cm^2 or 500 cells/cm^2 for colonies quantification and alkaline phosphatase assay, respectively, after 120 h in culture.

(B) Boxplot diagram (*left*) showing the number of domed-shaped colonies derived from control (untreated) and budesonide-treated dissociated gastruloids (n = 3; 15 fields/condition). Representative bright-field images of crystal violet and alkaline phosphatase (ALP)-stained colonies derived from control (untreated) and budesonide-treated dissociated gastruloids.

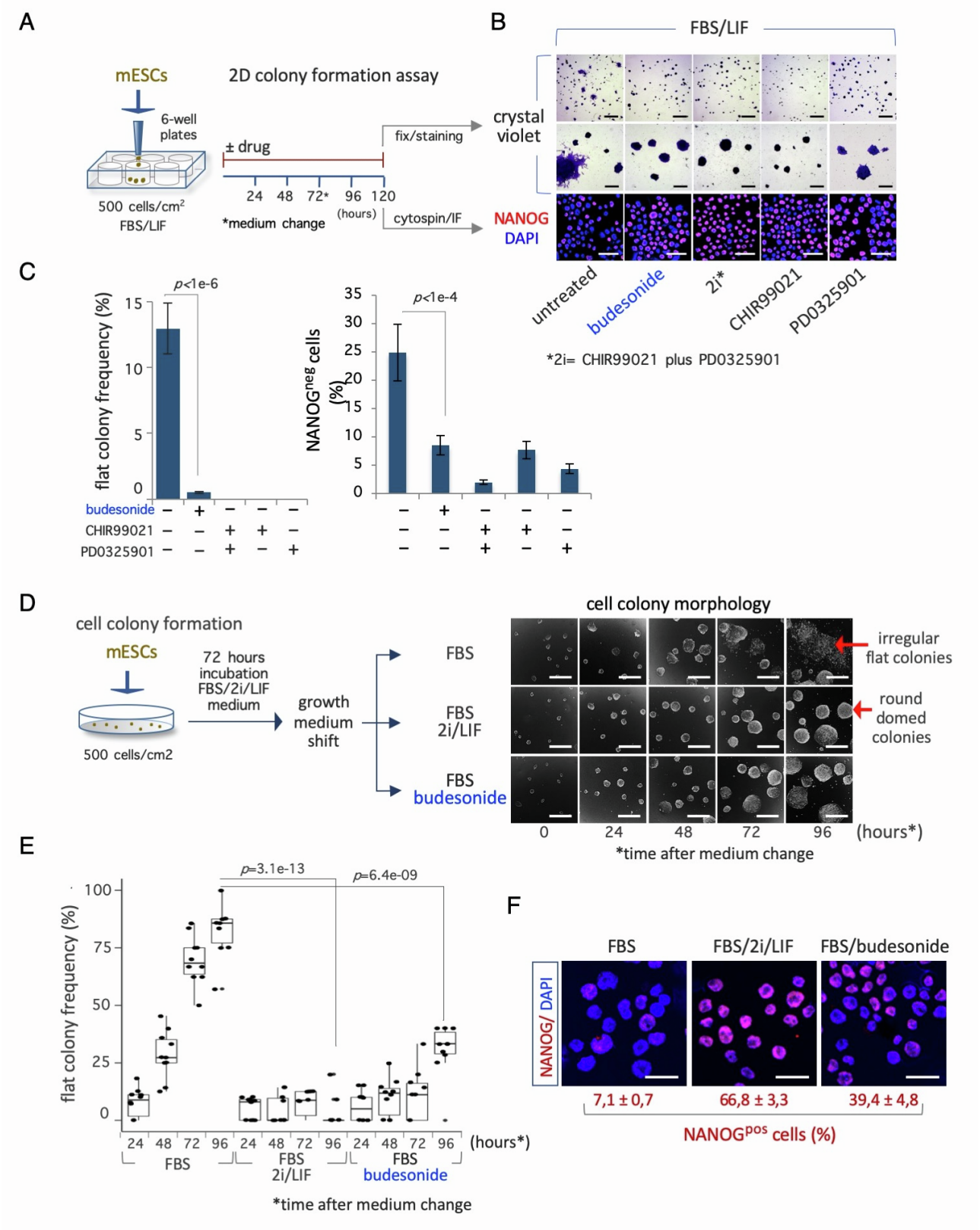

SUPPLEMENTARY FIGURE 6

Figure S6. Effect of budesonide on exit from naïve pluripotency.

(A) Schematic representation of the experimental design (*left*); ESCs were plated (500 cells/cm^2) and incubated in FBS/LIF medium ± budesonide, 2i, CHIR99021 or PD0325901. After 120 h in culture, cell colonies were either fixed and stained with crystal-violet or harvested and cytospinned.

(B) Representative bright-field images of crystal violet-stained cell colonies (*top*; bar, 200 μm) and representative confocal images (*bottom*) of NANOG expression on cytospin preparation in the different culture conditions. Nuclei were counterstained with DAPI (*blue*) (bar, 100 μm).

(C) Histogram showing the fraction (%) of flat-shaped cell colonies (*left*) and quantification of NANOG^{neg} cells in the different culture conditions (*right*). Data are mean ± SD (n = 3; 10 fields/condition)

(D) Schematic representation of the experimental design (*left*); ESCs were cultured in FBS/2i/LIF medium for 72 h and then shifted to either FBS alone, FBS + budesonide or maintained in FBS/2i/LIF as a control, and imaged every 24 h. Time course representative bright field images of the cell colonies in the different culture conditions (*right*; bar, 200 μm).

(E) Boxplot diagram showing the fraction (%) of irregular flat cell colonies generated from ESCs cultured in either FBS alone, FBS/2i/LIF or FBS + budesonide at the different time points (n=3; 10 fields/condition).

(F) Representative confocal images of NANOG (*red*) expression and quantification of NANOG^{pos} cells in cytospin preparation of ESCs cultured in the indicated conditions (n = 3; 30 fields/condition). Nuclei were counterstained with DAPI (*blue*) (bar, 50 μm).

Table S3. List of Primary and Secondary Antibodies used in this study, related to Figures 1, 2, 3, 6 and 7

Antibody	Source	Cat no.	Application
NANOG	Cell Signaling	8822	IF (1:400)
OCT4	Santa-Cruz	sc-8628	IF (1:100)
SOX2	Cell Signaling	D1C7J	IF (1:100)
CDX2	Cell Signaling	3977	IF (1:100)
E-CADHERIN	Takara	M108	IF (1:250)
BRACHYURY	Cell Signaling	D2Z3J	IF (1:500)
Alexa Fluor 594 Donkey anti-Rabbit IgG	Invitrogen	A21207	IF (1:400)
Alexa Fluor 594 Donkey anti-Goat IgG	Invitrogen	A11058	IF (1:400)
Alexa Fluor 647 Donkey anti-Rabbit IgG	Invitrogen	A31573	IF (1:400)
Alexa Fluor 488 Donkey anti-Rat IgG	Invitrogen	A21208	IF (1:400)
GR(M-20)	Santa-Cruz	sc-1004	WB (1:500)
GAPDH	Abcam	Ab8245	WB (1:40000)
Goat anti-Rabbit	DAKO	P0448	WB (1:2000)
Goat anti-Mouse	DAKO	P0447	WB (1:10000)

Table S4: List of Primers used in this study, Related to Figure 4

Gene symbol	Forward (5’-3’)	Reverse (5’-3’)
Nr3c1	ACTCTACCCTGCATGTATGACC	ACTCTTGGCTCTTCAGACCTTC

EXPERIMENTAL PROCEDURE

Gastruloid formation assay (GFA)

At 48 hours after aggregation, CHIR99021 was added to the culture medium at the concentration of 3 μM, or at the indicated concentrations, and maintained for 24 hours. From 72 hours onwards, the medium was refreshed daily up to 120 hours. Gastruloids were imaged using Levenhuk M300 Base Digital Camera for microscopes imaging systems, and the Confocal images were obtained on a Nikon A1 microscope.

To generate gastruloids from FBS/LIF ESCs + proline ± budesonide, ESCs were plated at low density on gelatin-coated plates in FBS/LIF medium supplemented with proline (500 μM) ± budesonide (10μM). After 120 h in culture, cells were dissociated with accutase and gastruloids formation assay was performed.

Western Blot

Total proteins were extracted in 100 mmol/L Tris pH 8, 140 mmol/L NaCl, 20 mmol/L EDTA, 0,2% SDS, 1% Nonidet P-40 lysis buffer, resolved on SDS-PAGE gels and transferred onto PVDF membranes (iBlot dry Transfer System; Life Technologies). Primary Antibodies were incubated ON at 4°C followed by HRP-conjugated secondary antibodies. Detection was performed with ECL reagents (Pierce, Thermo Scientific). ImageJ software was used for the densitometric analysis.